

Lawrence Berkeley National Laboratory

Lawrence Berkeley National Laboratory

Title

Detailed structural characterization of the grafting of $[Ta(=CHtBu)(CH_2tBu)_3]$ and $[Cp^*TaMe_4]$ on silica partially dehydroxylated at 700°C and the activity of the grafted complexes toward alkane metathesis

Permalink

<https://escholarship.org/uc/item/1wd4014f>

Authors

Le Roux, Erwan
Chabanas, Mathieu
Baudouin, Anne
et al.

Publication Date

2004-08-30

Peer reviewed

J|A|C|S

A R T I C L E S

Published on Web 00/00/0000

Detailed Structural Investigation of the Grafting of [Ta(=CH*t*Bu)(CH₂*t*Bu)₃] and [Cp*TaMe₄] on Silica Partially Dehydroxylated at 700 °C and the Activity of the Grafted Complexes toward Alkane Metathesis

Erwan Le Roux,^{†,‡} Mathieu Chabanas,^{†,‡} Anne Baudouin,[†] Aimery de Mallmann,[†]
Christophe Copéret,^{*,†} E. Alessandra Quadrelli,[†] Jean Thivolle-Cazat,[†]
Jean-Marie Basset,^{*,†} Wayne Lukens,[§] Anne Lesage,^{||} Lyndon Emsley,^{*,||} and
Glenn J. Sunley[⊥]

Contribution from the Laboratoire de Chimie Organométallique de Surface (UMR 9986
CNRS/ESCPE Lyon), ESCPE Lyon, F-308-43 Boulevard du 11 Novembre 1918,
F-69616 Villeurbanne Cedex, France, Chemical Sciences Division, Lawrence Berkeley National
Laboratory, Berkeley, California 94720, Laboratoire de Chimie (UMR 5532 CNRS/ENS),
Laboratoire de Recherche, Conventioonné du CEA (23V), Ecole Normale Supérieure de Lyon,
46 Allée d'Italie, F-69364 Lyon Cedex 07, France, and BP Chemicals Ltd., Hull Research and
Technology Center, Saltend, Hull, HU128DS, U.K.

Received June 14, 2004; E-mail: basset@cpe.fr; coperet@cpe.fr; lyndon.emsley@ens-lyon.fr

Abstract: The reaction of [Ta(=CH*t*Bu)(CH₂*t*Bu)₃] or [Cp*Ta(CH₃)₄] with a silica partially dehydroxylated at 700 °C gives the corresponding monosiloxy surface complexes [(=SiO)Ta(=CH*t*Bu)(CH₂*t*Bu)₂] and [(=SiO)Ta(CH₃)₃Cp*] by eliminating a σ-bonded ligand as the corresponding alkane (H–CH₂*t*Bu or H–CH₃). EXAFS data show that an adjacent siloxane bridge of the surface plays the role of an extra surface ligand, which most likely stabilizes these complexes as in [(=SiO)Ta(=CH*t*Bu)(CH₂*t*Bu)₂(=SiOSi=)] (**1a'**) and [(=SiO)Ta(CH₃)₃Cp*(=SiOSi=)] (**2a'**). In the case of [(=SiO)Ta(=CH*t*Bu)(CH₂*t*Bu)₂(=SiOSi=)], the structure is further stabilized by an additional interaction: a C–H agostic bond as evidenced by the small *J* coupling constant for the carbenic C–H (*J*_{C–H} = 80 Hz), which was measured by *J*-resolved 2D solid-state NMR spectroscopy. The product selectivity in propane metathesis in the presence of [(=SiO)Ta(=CH*t*Bu)(CH₂*t*Bu)₂(=SiOSi=)] (**1a'**) as a catalyst precursor and the inactivity of the surface complex [(=SiO)Ta(CH₃)₃Cp*(=SiOSi=)] (**2a'**) show that the active site is required to be highly electrophilic and probably involves a metallacyclobutane intermediate.

Introduction

The interaction of organometallic complexes with oxide surfaces such as silica or alumina has been studied for 30 years.^{1–5} The first application of these materials was to the generation of highly active heterogeneous polymerization catalysts, followed by applications to other catalytic processes such as hydrogenation, olefin and alkane metathesis, Fischer Tropsch, or oxidation. This approach is referred to as surface organometallic chemistry (SOMC), and its main objective is the transfer of concepts and tools from molecular chemistry to surface science.⁶ The recent development of advanced spectro-

scopic techniques has greatly helped to characterize the exact nature of active sites of these systems.^{7–10} Notably, we show how it is almost essential to combine the use of several analytical techniques to avoid making misleading conclusions. In this light, we discuss our results in comparison to previous studies carried out on these systems.¹¹ In the following study, we study and compare the reactivity of silica partially dehydroxylated at 700 °C with two tantalum complexes, [Ta(=CH*t*Bu)(CH₂*t*Bu)₃] and [Cp*TaMe₄]. The structure of each surface complex and the role of the silica surface on these structures will be discussed, highlighting the advantage of a rigorous multistep approach to

[†] Laboratoire de Chimie Organométallique de Surface, ESCPE Lyon.

[‡] Taken in part from his Ph.D. thesis.

[§] Lawrence Berkeley Laboratory.

^{||} Laboratoire de Chimie, ENS Lyon.

[⊥] BP Chemicals.

(1) Ballard, D. G. H. *Adv. Catal.* **1973**, *23*, 263–325.

(2) Yermakov, Y. I.; Kuznetsov, B. N.; Zakharov, V. A. *Stud. Surf. Sci. Catal.* **1981**, *8*, 522 pp.

(3) Basset, J. M.; Choplin, A. *J. Mol. Catal.* **1983**, *21*, 95–108.

(4) Evans, J. *NATO Adv. Study Inst. Ser., Ser. C* **1988**, *231*, 47–73.

(5) Scott, S. L.; Basset, J. M.; Niccolai, G. P.; Santini, C. C.; Candy, J. P.; Lecuyer, C.; Quignard, F.; Choplin, A. *New J. Chem.* **1994**, *18*, 115–122.

(6) Copéret, C.; Chabanas, M.; Petroff Saint-Arroman, R.; Basset, J.-M. *Angew. Chem., Int. Ed.* **2003**, *42*, 156–181.

(7) Petroff Saint-Arroman, R.; Chabanas, M.; Baudouin, A.; Copéret, C.; Basset, J.-M.; Lesage, A.; Emsley, L. *J. Am. Chem. Soc.* **2001**, *123*, 3820–3821.

(8) Chabanas, M.; Quadrelli, E. A.; Fenet, B.; Copéret, C.; Thivolle-Cazat, J.; Basset, J.-M.; Lesage, A.; Emsley, L. *Angew. Chem., Int. Ed.* **2001**, *40*, 4493–4496.

(9) Lesage, A.; Emsley, L.; Chabanas, M.; Copéret, C.; Basset, J.-M. *Angew. Chem., Int. Ed.* **2002**, *41*, 4535–4538.

(10) Chabanas, M.; Baudouin, A.; Copéret, C.; Basset, J.-M.; Lukens, W.; Lesage, A.; Hediger, S.; Emsley, L. *J. Am. Chem. Soc.* **2003**, *125*, 492–504.

(11) Ahn, H.; Marks, T. J. *J. Am. Chem. Soc.* **2002**, *124*, 7103–7110.

Table 1. Solid-State NMR Data for Solid **1**

ligand	$\delta^1\text{H/ppm}$	$\delta^{13}\text{C/ppm}$	$J_{\text{C-H/Hz}}$
=CHCMe ₃	4.2	247	80
=CHCMe ₃		47	
=CHCMe ₃	1.0	31	126
-CH ₂ CMe ₃	1.0	95	125
-CH ₂ CMe ₃		31	
-CH ₂ CMe ₃	1.0	31	126

53 surface organometallic chemistry. The choice of tantalum for
 54 such a study has been based on its unusual reactivity toward
 55 alkanes because alkane metathesis, a reaction which transforms
 56 an alkane into its higher and lower homologues, was originally
 57 discovered with [(≡SiO)₂Ta-H], a d² electron complex alkane
 58 metathesis catalyst.¹² We have recently disclosed that the
 59 mixture of [(≡SiO)Ta(=CH*t*Bu)(CH₂*t*Bu)₂] (**1a**) and
 60 [(≡SiO)₂Ta(=CH*t*Bu)(CH₂*t*Bu)] (**1b**), both d⁰ electron com-
 61 plexes, is also a catalyst precursor for this reaction.¹³ Because
 62 this study yielded two well-defined complexes, their activity in
 63 alkane metathesis was tested to gather information on the key
 64 requirements for an alkane metathesis catalyst precursors.

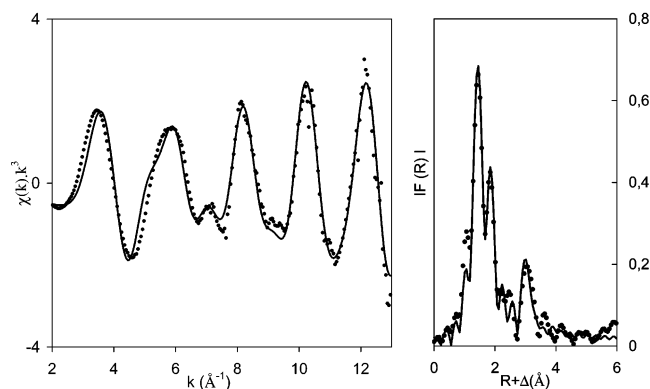
65 Results and Discussion

66 **Reactivity of [Ta(=CH*t*Bu)(CH₂*t*Bu)₃] with Silica Partially**
 67 **Dehydroxylated at 700 °C.** An exemplary case for multi-
 68 technique SOMC is given by the studies of the reactivity of
 69 [Ta(=CH*t*Bu)(CH₂*t*Bu)₃] with partially dehydroxylated silica.^{8,11,14,15} In the specific case of a silica partially dehydroxylated at 700 °C, the reaction leads to a yellow solid **1**, whose structure can be formulated as the well-defined monosiloxy Ta^V carbene [(≡SiO)Ta(=CH*t*Bu)(CH₂*t*Bu)₂], **1a**, as deduced by the combined use of mass balance analyses, IR, 1D and 2D HETCOR NMR spectroscopies (Table 1), and characterization through chemical reactivity studies (such as pseudo-Wittig or hydrolysis).

78 Furthermore, isotopic distribution studies¹⁴ and 1D solid-state
 79 NMR spectroscopy on selectively ¹³C-labeled complexes⁸ have
 80 indicated the involvement of the surface intermediate [(≡SiO)-
 81 Ta(CH₂*t*Bu)₄], **1c**, during the grafting reaction, and the slow
 82 transformation of **1c** into [(≡SiO)Ta(=CH*t*Bu)(CH₂*t*Bu)₂] **1a**
 83 and neopentane. The identification and characterization of **1c**,
 84 and the related mechanism of the grafting reaction, was further
 85 substantiated by studies of the reaction of the organometallic
 86 precursor with a molecular model for silica's surface isolated
 87 grafting site, the polyhedral oligosilsesquioxane [(*c*-C₅H₉)₇-
 88 Si₇O₁₂Si(OH)].⁸ Studies based solely on ¹³C solid-state NMR
 89 data for this reaction have postulated the same intermediate
 90 species, although NMR data have not always been correctly
 91 assigned.¹¹

92 Ideally, one would like to obtain crystallographic data to yield
 93 the interatomic geometric parameters of the coordination sphere
 94 of a metal center and its surroundings in the same way molecular
 95 chemists use X-ray crystallography diffraction studies on single
 96 crystals. In the case of silica, an amorphous support, extended
 97 X-ray absorption fine structure (EXAFS) analysis provides

- (12) Vidal, V.; Theolier, A.; Thivolle-Cazat, J.; Basset, J.-M. *Science* **1997**, *276*, 99–102.
 (13) Copéret, C.; Maury, O.; Thivolle-Cazat, J.; Basset, J.-M. *Angew. Chem., Int. Ed.* **2001**, *40*, 2331–2334.
 (14) Dufaud, V.; Nicolai, G. P.; Thivolle-Cazat, J.; Basset, J.-M. *J. Am. Chem. Soc.* **1995**, *117*, 4288–4294.
 (15) Lefort, L.; Chabanais, M.; Maury, O.; Meunier, D.; Copéret, C.; Thivolle-Cazat, J.; Basset, J.-M. *J. Organomet. Chem.* **2000**, *593–594*, 96–100.

**Figure 1.** EXAFS of solid **1**: dashed lines, experimental; solid lines, spherical wave theory.**Table 2.** EXAFS Parameters for Solid **1a**^a

neighboring atom	# of atoms ^b	distance (Å)	Debye–Waller factor (Å)
=CHCMe ₃	1	1.898(8)	0.07(6)
-OSi	1	1.898	0.03(2)
-CH ₂ CMe ₃	2	2.150(4)	0.07(2)
-OSi ₂	1	2.64(1)	0.11(4)
-CH ₂ CMe ₃	3	3.417(5)	0.06(2)

^a Fit residue: $\rho = 5.8\%$. ^b All shells fit with an overall scale factor of 1.1.

98 insight into the number and distances of first and second
 99 neighbors. The EXAFS data collected on the solid **1** are
 100 consistent with the following features (Figure 1 and Table 2):
 101 (i) two neighbors (either carbon or oxygen atoms) at a short
 102 distance (1.898 Å, not resolved), (ii) two other carbon neighbors
 103 at a longer distance (2.150 Å), (iii) an extra oxygen atom at
 104 a much longer distance (2.64 Å), and (iv) three carbon atoms at
 105 3.417 Å. The two neighbors at a short bond distance (1.898 Å)
 106 can be assigned to an alkylidene (=CH*t*Bu and a σ -bonded
 107 siloxy (OSi≡) substituent, while those at 2.150 Å are assigned
 108 to two σ -bonded carbons of the neopentyl groups (CH₂*t*Bu).
 109 The extra O-atom neighbor at 2.64 Å is assigned to a siloxane
 110 bridge which acts as a two-electron donor ligand to stabilize
 111 the otherwise highly electron unsaturated surface complex
 112 **1a** (formally a 10-electron complex) to yield the more sta-
 113 bilized 12-electron species [(≡SiO)Ta(=CH*t*Bu)(CH₂*t*Bu)₂-
 114 (≡SiOSi≡)], **1a'**.

115 The proposed ligand assignments for the observed bond
 116 distances are consistent with corresponding bond distances
 117 obtained by X-ray crystallography in analogous molecular
 118 complexes, such as $d(\text{Ta}=\text{CH}i\text{tBu}) = 1.89 \text{ \AA}$,^{16,17} $d(\text{Ta}-\text{C}) =$
 119 2.19 \AA ,¹⁸ $d(\text{Ta}-\text{OSi}) = 1.89 \text{ \AA}$,¹⁹ and $d(\text{Ta}\leftarrow\text{O}) = 2.25\text{--}2.35$
 120 \AA for a coordinated ether.^{20,21}

121 Recently, *J*-resolved 2D solid-state NMR spectroscopy was
 122 introduced as a novel method to measure the M–C–H bond
 123 angle and was applied to the study of surface-bound metallo-

- (16) Schrock, R. R. *Acc. Chem. Res.* **1979**, *12*, 98–104.
 (17) Schultz, A. J.; Brown, R. K.; Williams, J. M.; Schrock, R. R. *J. Am. Chem. Soc.* **1981**, *103*, 169–176.
 (18) LaPointe, R. E.; Wolczanski, P. T.; Van Duyne, G. D. *Organometallics* **1985**, *4*, 1810–1818.
 (19) Miller, R. L.; Toreki, R.; LaPointe, R. E.; Wolczanski, P. T.; Van Duyne, G. D.; Roe, D. C. *J. Am. Chem. Soc.* **1993**, *115*, 5570–5588.
 (20) Allen, K. D.; Bruck, M. A.; Gray, S. D.; Kingsborough, R. P.; Smith, D. P.; Weller, K. J.; Wigley, D. E. *Polyhedron* **1995**, *14*, 3315–3333.
 (21) Bott, S. G.; Sullivan, A. C. *J. Chem. Soc., Chem. Commun.* **1988**, 1577–1578.

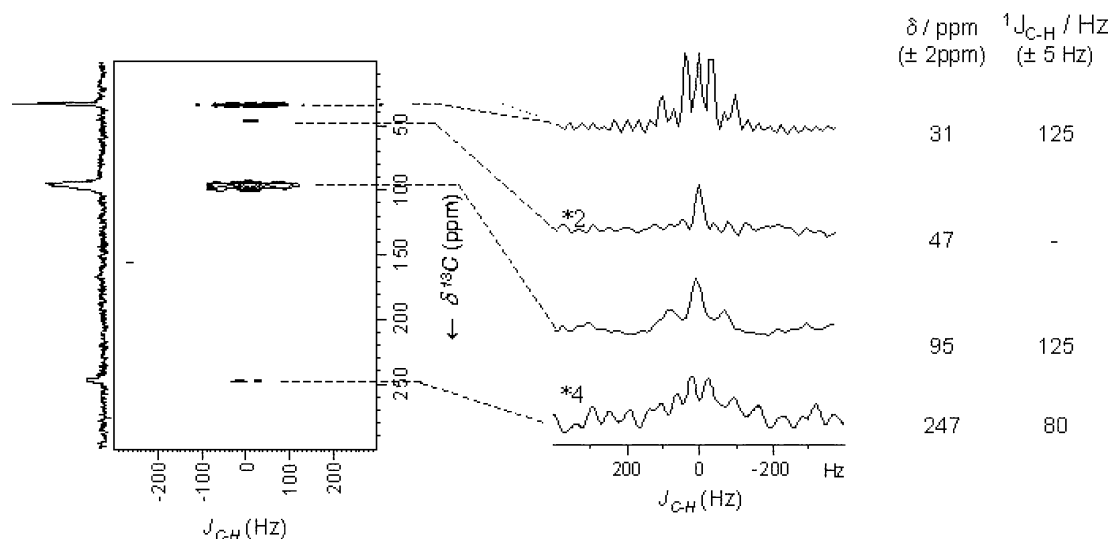
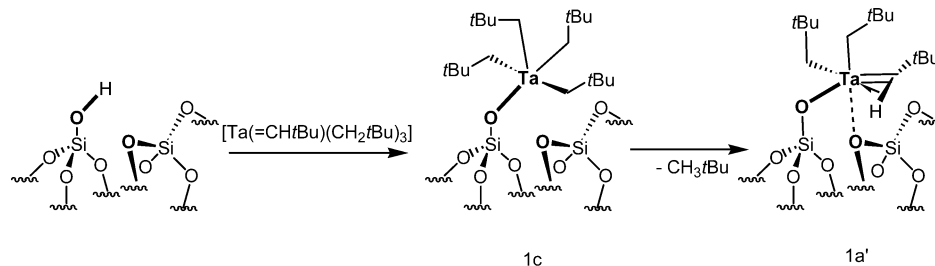


Figure 2. 2D J -resolved solid-state NMR spectrum of solid **1**, 10% ^{13}C enriched at the α positions (*). Traces extracted along the ω_1 dimension of the 2D J -resolved spectrum at different carbon chemical shift frequencies: 31, 47, 95, and 247 ppm.

Scheme 1. Reactivity of $[\text{Ta}(\text{=CH}t\text{Bu})(\text{CH}_2t\text{Bu})_3]$ with $\text{SiO}_2\text{-(700)}$; Formation of $[\text{=SiO-Ta}(\text{=CH}t\text{Bu})(\text{CH}_2t\text{Bu})_2(\text{=SiOSi=})]$ (**1a'**)



carbenes⁹ because their $J(\text{C-H})$ coupling constant is strongly correlated with this angle.^{16,22,23}

The results of the J -resolved 2D solid-state NMR study of **1a'** are reported in Table 2 and Figure 2.

The carbenic signal at 247 ppm appears as a doublet with a very small coupling constant of $^1J_{\text{C-H}} = 80$ Hz, strongly indicating that the C-H bond is stretched and that the Ta-C-H bond angle is very acute (probably lower than 90°). Similarly, the molecular silsesquioxane analogue, $[(\text{C-C}_5\text{H}_9)_7\text{-Si}_7\text{O}_{12}\text{SiO}]\text{Ta}(\text{=CH}t\text{Bu})(\text{CH}_2t\text{Bu})_2$ (**1m**), also displays a doublet ($J_{\text{C-H}} = 86$ Hz) at 245 ppm assigned to its carbenic carbons. Because similar spectroscopic features have been observed for the starting molecular complex, and explained in terms of an agostic interaction between the metallic center and the carbenic proton,^{16,24-26} we propose that the same type of agostic interaction is also present for the surface-bound Ta center and its α -carbenic proton of **1a'**.

The signal at 95 ppm, assigned to methylene (CH_2tBu), is a triplet, with C-H coupling constant $^1J_{\text{C-H}} = 125$ Hz, as expected for an sp^3 carbon. The molecular complex **1m** exhibits the analogous signal at 98.7 ppm (triplet, $^1J_{\text{C-H}} = 109$ Hz). In addition, there is a sharp singlet at 40 ppm, which can be

assigned to the quaternary carbon of the tert-butyl group attached to the carbene ligand; one other multiplet can be observed at 30 ppm, this resonance corresponding probably to the superimposition of a quadruplet ($^1J_{\text{C-H}} = 125$ Hz) due to the methyl signals and a singlet due to the quaternary carbon of the neopentyl ligands.

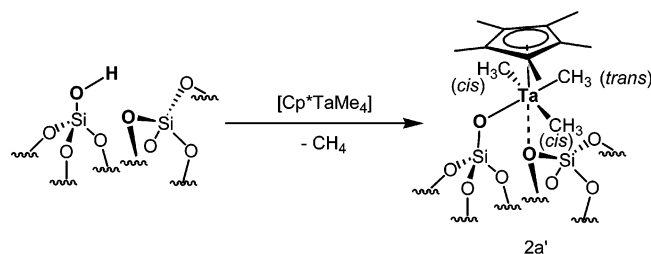
The combined use of EXAFS, IR, mass balance analyses, NMR studies (including $^1J_{\text{C-H}}$ -resolved data), and studies with molecular analogues yields a sharp description of the grafting reaction of organometallic precursor $[\text{Ta}(\text{=CH}t\text{Bu})(\text{CH}_2t\text{Bu})_3]$ on a silica surface (see Scheme 1).

Particularly noteworthy, the EXAFS and J -resolved studies have highlighted the presence of stabilizing interactions at the Ta-center, beside the σ -bonded alkyl and alkylidene ligands, with which the tantalum center (formally a tetracoordinated 10-electron species, **1a**) achieves a pseudo-octahedral geometry through (i) a 2-electron donor interaction with an adjacent (=SiOSi=) surface bridge, and (ii) an agostic interaction with the carbenic C-H bond, to yield the stabilized formally 14-electron species, $[(\text{=SiO})\text{Ta}(\text{=CH}t\text{Bu})(\text{CH}_2t\text{Bu})_2(\text{=SiOSi=})]$, **1a'**.

Reactivity of $[\text{Cp}^*\text{TaMe}_4]$ with Silica Partially Dehydroxylated at 700 °C. The reports available on the reactivity of Cp^*TaMe_4 (Scheme 2) with partially dehydroxylated silica are comprised of spectroscopic ^1H - and ^{13}C -CP NMR studies.¹¹ The data suggest that the organometallic surface species $[(\text{=SiO})\text{TaCp}^*\text{Me}_3]$, **2a**, is obtained, either by reaction with surface silanol (=SiOH) and elimination of methane, or by cleavage of a surface siloxy bridge [=SiOSi=] and formation

- (22) Brookhart, M.; Green, M. L. H. *J. Organomet. Chem.* **1983**, *250*, 395-408.
 (23) Nugent, W. A.; Mayer, J. M. *Metal-Ligand Multiple Bond*; Wiley: New York, 1988.
 (24) Schultz, A. J.; Williams, J. M.; Schrock, R. R.; Rupprecht, G. A.; Fellmann, J. D. *J. Am. Chem. Soc.* **1979**, *101*, 1593-1595.
 (25) Goddard, R. J.; Hoffmann, R.; Jemmis, E. D. *J. Am. Chem. Soc.* **1980**, *102*, 7667-7676.
 (26) Fellmann, J. D.; Schrock, R. R.; Traficante, D. D. *Organometallics* **1982**, *1*, 481-484.

Scheme 2. Reactivity of $[\text{Cp}^*\text{Ta}(\text{CH}_3)_4]$ with $\text{SiO}_2-(700)$: Formation of $[\equiv\text{SiO}-\text{Ta}(\text{CH}_3)_3\text{Cp}^*(\equiv\text{SiOSi}\equiv)]$ (**2a**)



175 of silicon bound methyl moiety, $[\equiv\text{Si}-\text{Me}]$. The presence of
176 this latter species is inferred by one signal at -6 ppm in the
177 ^{13}C NMR spectrum.¹¹

178 Herein is discussed in detail the reaction of $[\text{Cp}^*\text{TaMe}_4]$ with
179 a silica partially dehydroxylated at 700°C . First, a silica disk
180 partially dehydroxylated at 700°C ($\text{SiO}_2-(700)$) was immersed
181 at room temperature in a yellow pentane solution of $[\text{Cp}^*\text{TaMe}_4]$ -
182 (1.2 equiv/surface silanols; 0.26 ± 0.03 mmol accessible OH/
183 g). After the excess molecular complex was washed and the
184 resulting solid was dried under dynamic vacuum (10^{-5} Torr, 2
185 h), an IR spectrum was recorded (Figure 3).

186 The narrow band assigned to isolated silanols at 3747 cm^{-1}
187 totally disappeared, leaving a broad band in the $3740\text{--}3550$
188 cm^{-1} region as well as two sets of bands in the $3000\text{--}2700$
189 and $1500\text{--}1300\text{ cm}^{-1}$ regions. The broad band corresponds to
190 $\nu_{(\text{O}-\text{H})}$ of residual silanols in interaction with the perhydrocarbyl
191 ligands present at the surface of silica (vide infra for further
192 comments), the two latter sets of IR bands being assigned to
193 $\nu_{(\text{CH})}$ and $\nu_{(\text{C}=\text{C})}/\delta_{(\text{CH})}$ vibrations.

194 Second, using larger quantities of silica (0.20–1.0 g) allowed
195 the methane released to be quantified: 1.1–1.2 equiv of methane
196 was evolved per grafted Ta, consistent with a chemical grafting
197 of the molecular complex. This reaction occurs via cleavage of
198 one (Ta–CH₃) bond by a surface silanol forming a covalent
199 (Ta–Osi≡) bond and methane to yield a yellow solid **2**. The
200 formation of $[(\equiv\text{SiO})\text{TaCp}^*\text{Me}_3]$, **2a**, leads to 1 mol of MeH/
201 mol of grafted Ta as expected, and therefore small quantities
202 of the bisiloxy species $[(\equiv\text{SiO})_2\text{TaCp}^*\text{Me}_2]$, **2b**, for which 2
203 mol of MeH/mol of grafted Ta are expected, could also be
204 possibly formed. Elemental analysis of the yellow solid shows
205 the presence of 12 ± 2 carbons/Ta, which is consistent with
206 the proposed structure (13 C/Ta and 12 C/Ta for **2a** and **2b**,
207 respectively). The tantalum loading typically varies between 2.6
208 and 3.7 Ta % wt, depending on the batch of $\text{SiO}_2-(700)$ used
209 (depending on how much silica was compacted). Such tantalum
210 loadings correspond to 0.14–0.21 mmol of Ta/g of solid, while
211 $\text{SiO}_2-(700)$ typically contains 0.26 ± 0.03 mmol of OH/g on
212 silica. Therefore, such low loading indicates a partial consump-
213 tion of the surface silanols as already evidenced by in situ IR
214 experiments (vide supra) where a broad band assigned to
215 residual silanols was detected. This is in contrast to what has
216 been observed in the reaction of $[\text{Ta}(\equiv\text{CH}t\text{Bu})(\text{CH}_2t\text{Bu})_3]$ with
217 $\text{SiO}_2-(700)$,¹⁵ for which all surface silanols are consumed, but it
218 is consistent with the larger size of the $[\text{TaCp}^*\text{Me}_3]$ fragment
219 as compared to that of $[\text{Ta}(\equiv\text{CH}t\text{Bu})(\text{CH}_2t\text{Bu})_2]$, which, in turn,
220 would prevent the access of the molecular complex, $[\text{Cp}^*\text{TaMe}_4]$,
221 to the remaining surface silanols.

222 Third, the solid-state ^1H MAS NMR spectrum of the yellow
223 solid **2** shows an intense peak at 1.61 ppm along with broad
224 signals between -0.3 and 0.7 ppm, as does the ^1H spectrum of

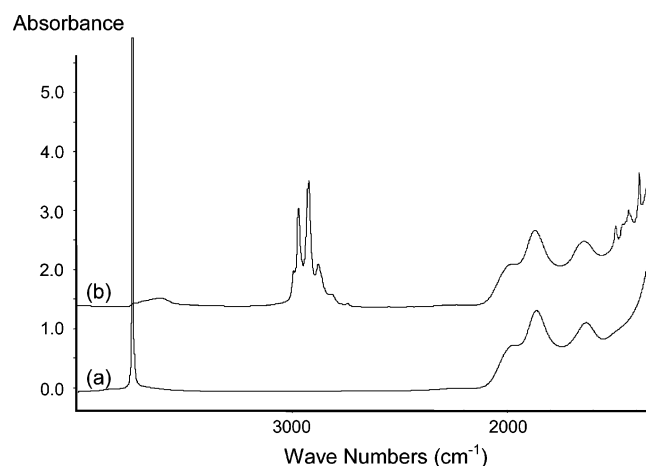


Figure 3. IR spectra of the reaction of $[\text{Cp}^*\text{Ta}(\text{CH}_3)_4]$ with $\text{SiO}_2-(700)$ by IR spectroscopy: (a) $\text{SiO}_2-(700)$ and (b) $[\equiv\text{SiO}-\text{Ta}(\text{CH}_3)_3\text{Cp}^*(\equiv\text{SiOSi}\equiv)]$.

225 its ^{13}C -labeled (20% on the Me substituents attached to Ta)
226 analogue, **2*** (Figure 4a). The ^{13}C CP/MAS NMR spectrum of
227 **2** displays three signals at 117, 58, and 9 ppm, as does the
228 spectrum of **2*** (albeit with different relative ratios, Figure 4b).
229 In accord with the literature data,¹¹ the signals at 117 and 9
230 ppm can be tentatively assigned to the carbons of the cyclo-
231 pentadienyl ring and the methyl groups of the Cp^* ligand,
232 respectively, and the signal at 58 ppm can be assigned to that
233 of the (Ta–Me₃) groups, which is shifted upfield as compared
234 to that of the starting molecular complex $[\text{Cp}^*\text{TaMe}_4]$ (Ta–
235 Me₄, 74 ppm). The large upfield shift in going from a molecular
236 to a supported complex is consistent with the replacement of
237 one methyl group by an electronegative siloxy group.^{27,28} No
238 resonance of any significance could be detected at -6 ppm,
239 which is the signature peak of $[\equiv\text{Si}-\text{Me}]$ as previously
240 reported,¹¹ and no further evidence for a bisiloxy species could
241 be obtained through these NMR studies.

242 Fourth, the 2D $^1\text{H}-^{13}\text{C}$ HECTOR NMR spectrum of **2***,
243 recorded with a contact time of 1 ms (Figure 4c), shows a
244 correlation between the signal at 1.6 ppm in the F_1 dimension
245 (^1H) and the signal at 9 ppm in the F_2 dimension (^{13}C), which
246 are assigned to the methyl groups of the pentamethylcyclopent-
247 adienyl ring. The ^{13}C resonance of the methyl groups directly
248 bonded to the tantalum gives two pairs of correlations: -0.05
249 ppm/58.0 ppm and -0.28 ppm/57.5 ppm in the F_1/F_2 dimen-
250 sions. These two types of proton–carbon resonances probably
251 correspond to the methyl group trans to oxygen (58.0 and -0.05
252 ppm), and the other correlation (57.5 and -0.28 ppm) corre-
253 sponds to the cis methyl groups as observed for similar
254 molecular complexes, $\text{Cp}^*\text{TaXMe}_3$ (X = Cl, OMe, OiPr, OtBu,
255 NMe₂), which adopt a “four-legged piano stool” geometry and
256 in which the two types of methyl groups are not equivalent.²⁷
257 The signal at 0.6 ppm in the F_1 dimension (^1H) does not correlate
258 with any carbon (in the F_2 dimension), and this signal disappears
259 when using deuterated silica (see Supporting Information).
260 Therefore, the resonance at 0.6 ppm is most likely due to a
261 surface silanol $[\equiv\text{SiO}-\text{H}]$ resonance, which is shifted upfield

(27) Mayer, J. M.; Curtis, C. J.; Bercaw, J. E. *J. Am. Chem. Soc.* **1983**, *105*, 2651–2660.

(28) Gomez, M.; Jimenez, G.; Royo, P.; Selas, J. M.; Raithby, P. R. *J. Organomet. Chem.* **1992**, *439*, 147–154.

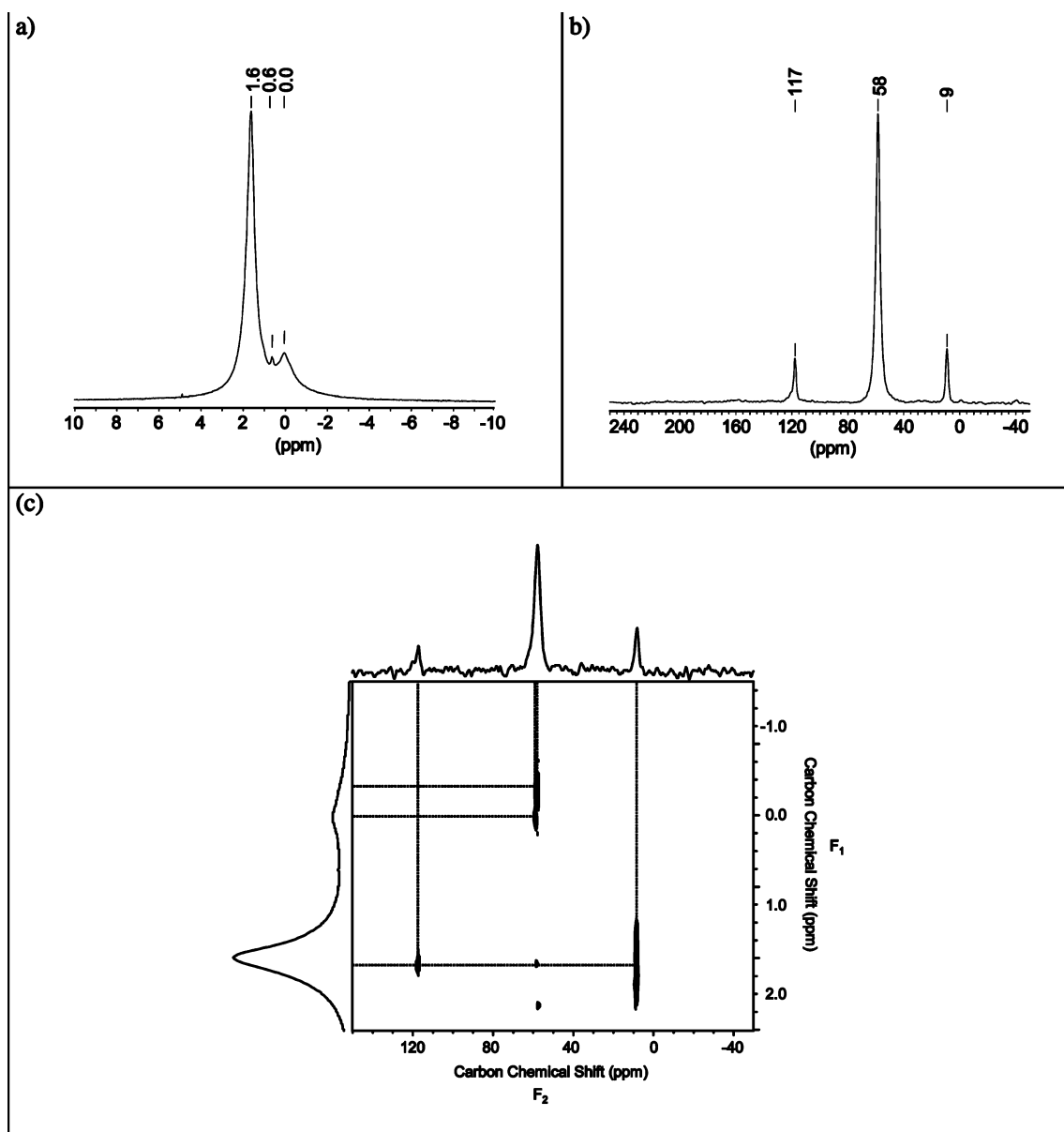


Figure 4. (a) ^1H MAS NMR spectrum of **2*** (number of scans = 8, repetition delay = 8 s, 90° H pulse = $3\ \mu\text{s}$, no apodization). (b) ^{13}C CP/MAS spectrum of **2*** (number of scans = 78 339, repetition delay = 2 s, P15 = 5 ms, line broadening = 100 Hz). (c) 2D HETCOR solid-state NMR spectroscopy on **2***. The displayed spectra correspond to a ^1H MAS NMR spectrum (number of scans = 16, repetition delay = 8 s, line broadening = 5 Hz) for F_1 and ^{13}C CP/MAS spectrum (number of scans = 1024, repetition delay = 2 s, P15 = 1 ms, line broadening = 80 Hz) for F_2 .

with respect to the silanols of silica (typically observed at 1.8 ppm), most likely because of a ring-current effect of the adjacent Cp^* ring.

Finally, Tantalum L_{III} -edge EXAFS measurements on **2** provided further insight into the structure of this silica-supported Ta species (Figure 5).

The data are consistent with an average of 1.3 oxygen atoms at 1.931 Å, 2.7 carbon atoms at 2.142 Å, and 5.0 carbon atoms at 2.456 Å in the coordination sphere of Ta, which is in turn consistent with **2a** being the major species present in the solid, and **2b** (if any) as a minor product (Table 3).

The proposed assignment for measured Ta–C bond distances is in good agreement with values obtained from crystallographic data for Ta–C(Me) (2.074–2.150 Å in $[\text{TaMe}_5]$;²⁹ 2.115 Å in

$[\text{TaMe}_3(\text{OAr})_2]$;³⁰ 2.181 Å in $[\text{Cp}^*\text{TaMe}_2(\text{C}_6\text{H}_4)]$;³¹ and 2.22–2.26 Å in $[(\text{TaMe}_3\text{Cp}^*)_2(\mu\text{-O})]$ ³²) and Ta–C(pentamethylcyclopentadienyl) distances (2.345–2.406 Å in $[\text{Cp}^*\text{TaCl}_2\text{Me}_2]$;²⁸ 2.424–2.480 Å in $[\text{Cp}^*\text{Ta}(p\text{-tert-butylcalix[4]arene})]$;³³ 2.366–2.518 Å in $[\text{Cp}^*\text{Ta}(=\text{NAr})\text{Cl}_2]$ ³⁴). Moreover, the agreement with the EXAFS data was improved when the model included five carbons at 3.44 Å, corresponding to the five methyl groups of the Cp^* ligand (3.42–3.61 Å in $[\text{Cp}^*\text{Ta}(=\text{NAr})\text{Cl}_2]$ ³⁴), and an extra 1.3 oxygen atoms at 3.04 Å, which can be assigned to that of siloxane bridges close to a tantalum species, to yield

(30) Chamberlain, L. R.; Rothwell, I. P.; Huffman, J. C. *J. Am. Chem. Soc.* **1986**, *108*, 1502–1509.

(31) Churchill, M. R.; Youngs, W. J. *Inorg. Chem.* **1979**, *18*, 1697–1702.

(32) Jernakoff, P.; De Meric de Bellefon, C.; Geoffroy, G. L.; Rheingold, A. L.; Geib, S. J. *Organometallics* **1987**, *6*, 1362–1364.

(33) Acho, J. A.; Doerrer, L. H.; Lippard, S. J. *Inorg. Chem.* **1995**, *34*, 2542–2556.

(34) Gavenonis, J.; Tilley, T. D. *Organometallics* **2004**, *23*, 31–43.

(29) Roessler, B.; Kleinhenz, S.; Seppelt, K. *Chem. Commun.* **2000**, 1039–1040.

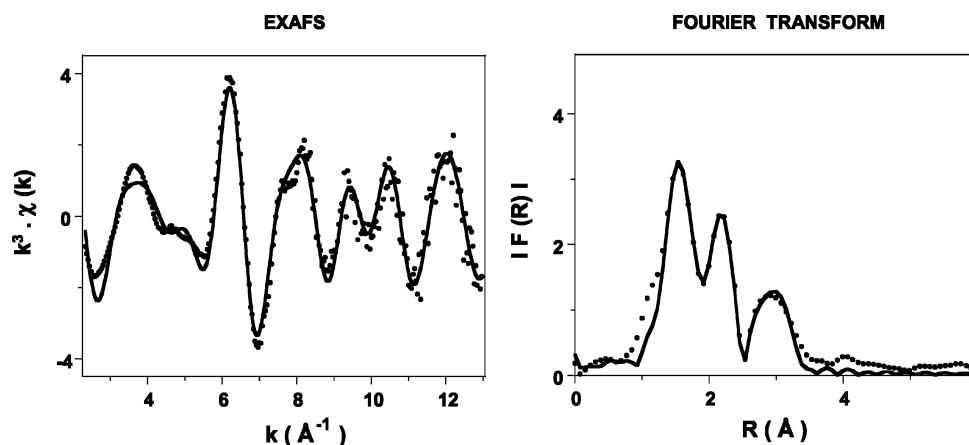


Figure 5. Ta L_{III}-edge k³-weighted EXAFS (left) and Fourier transform (right) of **2**. Dashed lines, experimental; solid lines, spherical wave theory.

Table 3. EXAFS Parameters for Solid **2**^a

neighboring atom	# of atoms	distance from Ta (Å)	Debye–Waller factor (Å)
OSi	1.3	1.931	0.042
CH ₃	2.7	2.142	0.097
C' (Cp* ring)	5.0	2.456	0.086
OSi ₂	1.3	3.040	0.063
C'' (Me of Cp*)	4.8	3.445	0.082

^a Fit residue: $\rho = 7.8\%$.

286 [(≡SiO)TaCp*Me₃(≡SiOSi≡)], **2a'**, analogous to the observa-
287 tions for the carbenic derivative discussed above [(≡SiO)Ta-
288 (≡CH*t*Bu)(CH₂*t*Bu)₂(≡SiOSi≡)], **1a'**.

289 In summary, the combined analysis of the experimental data
290 collected on the reaction of Cp*TaMe₄ with SiO₂-(700) indicates
291 the presence of [(≡SiO)TaMe₃Cp*(≡SiOSi≡)] (**2a'**) as a major
292 species, in which a siloxane bridge acts as an extra donor ligand
293 to the Ta center. In contrast to most organometallic complexes
294 studied so far, only part of the surface silanols reacted with
295 [Cp*TaMe₄], as demonstrated by elemental analysis, IR, and
296 NMR spectroscopies. The remaining silanols interact with a
297 nearby Cp* as observed through the upfield shift of δ (≡SiOH)
298 in the ¹H NMR spectrum. The grafting mechanism corresponds
299 to the silanolysis of a Ta–Me bond by a surface [≡SiOH], with
300 elimination of 1 mole of methane, while no evidence was
301 obtained supporting the previously proposed addition of a Ta–C
302 across a Si–O bond of a surface siloxy bridge [≡SiOSi≡].¹¹

303 **Comparison of the Reactivity of [Cp*TaMe₄] and**
304 **[Ta(≡CH*t*Bu)(CH₂*t*Bu)₃] Supported on Silica Partially De-**
305 **hydroxylated at 700 °C toward Propane.** In the case of
306 [(≡SiO)Ta(CH₃)₃Cp*(≡SiOSi≡)] (**2a'**), a sterically crowded
307 electron-rich Ta^V surface complex, its reaction with propane
308 yields methane as the sole gaseous product, which probably
309 formed via the decomposition of **2a'** (Table 4). On the other
310 hand, [(≡SiO)Ta(≡CH*t*Bu)(CH₂*t*Bu)₂(≡SiOSi≡)] (**1a'**), an
311 electron-deficient Ta^V surface complex as evidenced by the
312 C–H agostic interaction, catalytically transforms propane into
313 its higher and lower homologues (Table 4). Moreover, initiation
314 products, which result from the reaction of the neopentyl/
315 neopentylidene fragments in **1a'** and propane, are also formed:
316 2,2-dimethylpropane (*t*BuCH₂-H, 1.05 equiv/Ta), 2,2-dimeth-
317 ylbutane (*t*BuCH₂-CH₃, 0.30 equiv/Ta), and 2,2-dimethylpentane
318 (*t*BuCH₂-CH₂CH₃, 0.11 equiv/Ta). Note that no *t*BuCH₂-
319 CH₂CH₂CH₃ (<0.1%, not detected) is formed. The ratio of
320 initiation products *t*BuCH₂-CH₃/*t*BuCH₂-CH₂CH₃ is 2.5. Simi-

Table 4. Reactivity of Tantalum Species Supported on Silica toward Propane

catalysts	% wt Ta	<i>P</i> (Torr)	ratio (nC ₃ H ₈ /nTa)	conv. ^a (%)	TON ^a (mol P/mol Ta)
solid 2	3.5	495	805	0	0
solid 1	3.9	600	580	5.8	33–34 ^b
[(≡SiO) ₂ Ta–H]	5.0	550	1065	6.1	65 ^c

^a As measured after 120 h. ^b The selectivities in methane, ethane, isobutane, butane, isopentane, pentane, and hexanes are 12.8%, 47.7%, 10.2%, 22.2%, 2.5%, 3.6%, and 0.9%, respectively. ^c The selectivities in methane, ethane, isobutane, butane, isopentane, pentane, and hexanes are 18.0%, 40.0%, 8.6%, 24.4%, 2.9%, 5.1%, and 1%, respectively.

321 larly in olefin metathesis (Scheme 3), we have observed the
322 initiation products of the reaction of propene and [(≡SiO)Re-
323 (≡C*t*Bu)(≡CH*t*Bu)(CH₂*t*Bu)(≡SiOSi≡)]: *t*BuCH=CH₂ and
324 *trans-t*BuCH=CHCH₃ (no *cis-t*BuCH=CHCH₃ is detected).^{35,36}
325 Their ratio (*t*BuCH=CH₂/*trans-t*BuCH=CHCH₃) is 3.0, which
326 is closely related to that observed for the initiation products
327 in the metathesis of propane on [(≡SiO)Ta(≡CH*t*Bu)(CH₂*t*Bu)₂-
328 (≡SiOSi≡)] (**1a'**). In this latter case, the selectivity in initiation
329 products can be understood in terms of minimization of the steric
330 interactions in the metallacyclobutane intermediates (or in their
331 formation),³⁷ which is governed by the relative position of the
332 substituents: typically substituents in the [1,3]-positions (usually
333 both in equatorial positions) of the metallacyclobutane inter-
334 mediate generate less steric hindrance than those in the [1,2]-
335 positions (usually both in equatorial positions, Scheme 3).³⁸

336 The selectivity in propane metathesis can also be explained
337 by using the same model in which [1,3]- and [1,2]-interactions
338 determine the ratio of products. For instance, the butane/pentane
339 ratios are 6.2 and 4.8 for **1a'** and [(≡SiO)₂Ta–H], respectively
340 (Table 4).³⁹ A similar trend is observed for the isobutane/
341 isopentane ratios, which are 4.1 and 3.0, respectively. The higher
342 selectivity in butanes (the transfer of one carbon via metalla-
343 cyclobutanes involving [1,3]-interactions) than that of pentanes

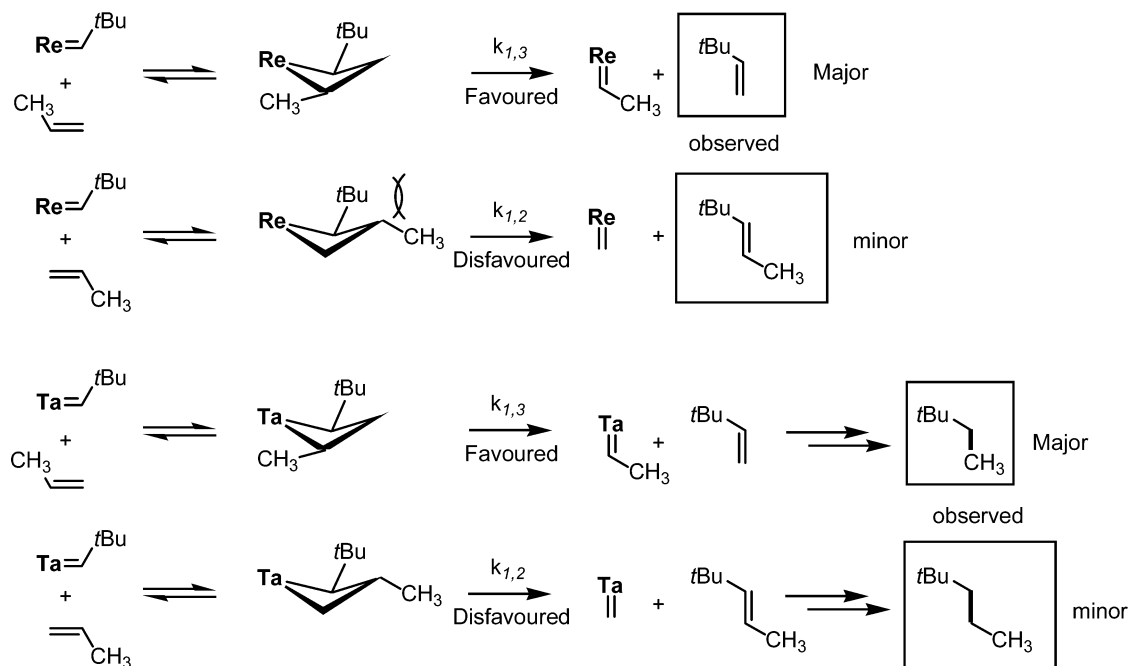
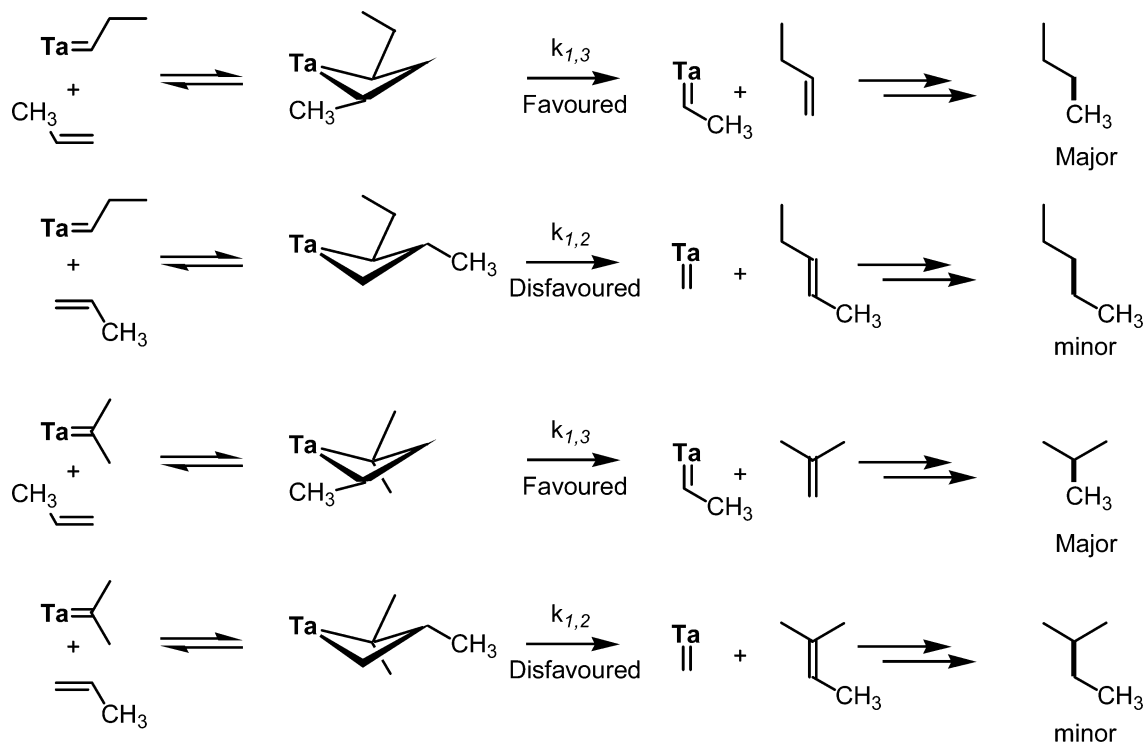
(35) Chabanas, M.; Baudouin, A.; Copéret, C.; Basset, J.-M. *J. Am. Chem. Soc.* **2001**, *123*, 2062–2063.

(36) Chabanas, M.; Copéret, C.; Basset, J.-M. *Eur. J. Chem.* **2003**, *9*, 971–975.

(37) Wallace, K. C.; Dewan, J. C.; Schrock, R. R. *Organometallics* **1986**, *5*, 2162–2164.

(38) Bilhou, J. L.; Basset, J. M.; Mutin, R.; Graydon, W. F. *J. Am. Chem. Soc.* **1977**, *99*, 4083–4090.

(39) In the case of Ta–H, this ratio does not change with time, while the isobutane/butane ratio decreases in the case of [(≡SiO)Ta(≡CH*t*Bu)(CH₂*t*Bu)₂] because isobutane is also formed through the decomposition of this complex at 150 °C.

Scheme 3. Possible Relation between the Mechanisms of Olefin and Alkane Metatheses: The Initiation Step**Scheme 4.** Model for Product Selectivities in Alkane Metathesis

344 (the transfer of two carbons via metallacyclobutanes involving
 345 [1,2]-interactions) is consistent with this model (Schemes 3 and
 346 4).

347 Because alkane metathesis catalysts need to be highly
 348 electrophilic and coordinatively unsaturated (Cp^* is detrimental
 349 to catalysis), because the selectivities of initiation products and
 350 alkane metathesis products are similar to that observed for olefin
 351 metathesis, and because $\mathbf{1a}'$, a metalcarbene, is a catalyst
 352 precursor for alkane metathesis, we therefore propose that one
 353 of the key steps in alkane metathesis would be the formation
 354 of a metallacyclobutane intermediate and probably involves

metallocarbenes rather than direct C–C σ -bond metathesis or
 oxidative addition pathways as was suggested earlier as a
 possible working hypothesis.

Experimental Details

General Procedure. All experiments were carried out under a
 controlled atmosphere, using Schlenk and glovebox techniques for the
 organometallic synthesis. For the synthesis and treatments of the surface
 species, reactions were carried out using high-vacuum lines (1.34 Pa)
 and glovebox techniques. SiO_2 (Aerosil Degussa, $200 \text{ m}^2 \text{ g}^{-1}$) was
 compacted with distilled water, calcined ($500 \text{ }^\circ\text{C}$ under air for 4 h),

and partially dehydroxylated under vacuum (1.34 Pa) at 500 °C for 12 h and then at 700 °C for 4 h (support referred to as SiO₂₋₍₇₀₀₎). [Ta(=CHtBu)(CH₂tBu)₃] and [Cp*Ta(CH₃)₃] were prepared according to the literature procedure.⁴⁰ The 10% ¹³C-labeled [Ta(=CHtBu)(CH₂tBu)₃] was prepared as reported previously.^{8,10} ¹³C-labeled Cp*Ta(CH₃)₃ was prepared following the literature procedure for the unlabeled complex, using ¹³CH₃Li prepared from Li wire and CH₃I.⁴¹ Pentane and diethyl ether were distilled on NaK alloy and Na/benzophenone, respectively followed by degassing through freeze–pump–thaw cycles. Infrared spectra were recorded on a Nicolet Magna 550 FT spectrometer equipped with a cell designed for in situ reactions under controlled atmosphere. Elemental analyses were performed at the Service Central d'Analyses of CNRS in Solaize.

¹H MAS and ¹³C CP-MAS solid-state NMR spectra were recorded on a Bruker DSX-300 spectrometer. For specific studies (see below), ¹H MAS and ¹³C CP-MAS solid-state NMR spectra were recorded on Bruker Avance-500 spectrometers with a conventional double resonance 4 mm CP-MAS probe at the Laboratoire de Chimie in Ecole Normale Supérieure de Lyon or at the Laboratoire de Chimie Organometallique de Surface in Ecole Supérieure de Chimie Physique Electronique de Lyon. The samples were introduced under Ar in a zirconia rotor, which was then tightly closed. In all experiments, the rotation frequency was set to 10 kHz unless otherwise specified. Chemical shifts were given with respect to TMS as external references for ¹H and ¹³C NMR.

Heteronuclear Correlation Spectroscopy. The two-dimensional heteronuclear correlation experiment was performed according to the following scheme: 90° proton pulse, *t*₁ evolution period, cross-polarization (CP) to carbon spins, detection of carbon magnetization. For the CP step, a ramp radio frequency (RF) field^{42,43} centered at 60 kHz was applied on protons, while the carbon RF field was matched to obtain optimal signal. The contact time for CP was set to 1 ms. During acquisition, the proton decoupling field strength was set to 83 kHz (TPPM decoupling⁴⁴). A total of 32 *t*₁ increments with 1024 scans each were collected. The spinning frequency was 10 kHz, and the recycle delay was 1 s (total acquisition time of 9 h). Quadrature detection in ω_1 was achieved using the TPPI method.⁴⁵

J-Resolved Spectroscopy. The two-dimensional *J*-resolved experiment was performed as previously described,⁹ after cross-polarization from protons, carbon magnetization evolves during *t*₁ under proton homonuclear decoupling. Simultaneous 180° carbon and proton pulses are applied in the middle of *t*₁ to refocus the carbon chemical shift evolution while retaining the modulation by the heteronuclear *J*_{CH} scalar couplings. A Z-filter is finally applied to allow phase-sensitive detection in ω_1 . Proton homonuclear decoupling was performed by using the frequency-switched Lee–Goldburg (FSLG) decoupling sequence.^{46,47} Quadrature detection in ω_1 was achieved using the TPPI method.⁴⁵ The rotor spinning frequency was 10.2 kHz to synchronize the *t*₁ increment with the rotor period. The proton RF field strength was set to 83 kHz during *t*₁ (FSLG decoupling) and acquisition (TPPM decoupling).⁴⁴ The lengths of carbon and proton 180° pulses were 7 and 6 μ s, respectively. An experimental scaling factor, measured as already described,⁴⁸ of 0.52 was found, which gave a corrected spectral width of 2452 Hz in

the ω_1 dimension. The recycle delay was 1.3 s, and a total of 80 *t*₁ increments with 1024 scans each were collected (total acquisition time = 30 h).

Extended X-ray Absorption Fine Structure Spectroscopy (EXAFS). EXAFS on **1a** was carried out at the Stanford Synchrotron Radiation Laboratory (SSRL) at beamline 4-1 as previously reported.¹⁰ Samples **2** was packaged within an argon-filled drybox in double airtight sample holders equipped with Kapton windows. X-ray absorption spectra were acquired at the Laboratoire pour l'Utilisation du Rayonnement Electromagnétique (LURE in Orsay, France), on the DCI ring at beam line D44. They were recorded at room temperature at the tantalum L_{III} edge, from 9700 to 11 000 eV, with a 2 eV step in the transmission mode. The data analysis was performed by standard procedures using either the suite of programs EXAFSPAK developed by G. George of SSRL or the one developed by A. Michalowicz.⁴⁹ Each spectrum was carefully extracted, and the best removal of low-frequency noise was checked by further Fourier transformation. Fitting of the spectrum was done on the *k*³ weighted data using the following EXAFS equation where *S*₀² is the scale factor; *N*_{*i*} is the coordination number of shell *i*; *S*_{*i*} is the central atom loss factor for atom *i*; *F*_{*i*} is the EXAFS scattering function for atom *i*; *R*_{*i*} is the distance to atom *i* from the absorbing atom; λ_i is the photoelectron mean free path; σ_i is the Debye–Waller factor; ϕ_i is the EXAFS phase function for atom *i*; and ϕ_c is the EXAFS phase function for the absorbing atom.

$$\chi(k) \cong S_0^2 \sum_{i=1}^n \frac{N_i S_i(k, R_i) F_i(k, R_i)}{k R_i^2} \exp\left(\frac{-2R_i}{\lambda(k, R_i)}\right) \times \exp(-2\sigma_i^2 k^2) \sin[2kR_i + \phi_i(k, R_i) + \phi_c(k)]$$

The program FEFF7⁵⁰ was used to calculate theoretical values for *S*_{*i*}, *F*_{*i*}, λ_i , ϕ_i , and ϕ_c based on model clusters of atoms in which atomic positions were taken from the crystal structure of the most similar complexes. The refinements were performed by fitting the structural parameters *N*_{*i*}, *R*_{*i*} and σ_i . The fit residue, ρ , was calculated by the following formula:

$$\rho = \frac{\sum_k [k^3 \chi_{\text{exp}}(k) - k^3 \chi_{\text{Cal}}(k)]^2}{\sum_k [k^3 \chi_{\text{exp}}(k)]^2}$$

Reaction of Silica Partially Dehydroxylated at 700 °C with [Ta(CHtBu)(CH₂tBu)₃], Formation of the Solid 1. A mixture of [Ta(CHtBu)(CH₂tBu)₃] (0.155 g, 0.33 mmol) in pentane (10 mL) and SiO₂₋₍₇₀₀₎ (1.0 g) was stirred at 25 °C for 2 h. After filtration, the solid was washed three times with pentane. The solvent was then removed, and the yellow orange solid was dried under dynamic-vacuum at 25 °C.

Reaction of Silica Partially Dehydroxylated at 700 °C with [Cp*TaMe₄]: Formation of the Solid 2. A mixture of Cp*TaMe₄ (42.5 mg, 0.11 mmol, 1.2 equiv) and SiO₂₋₍₇₀₀₎ (373 mg) in pentane (5 mL) was stirred at 25 °C for 2 h. After filtration, the solid was washed three times with pentane and all volatile compounds were condensed into another reactor (of known volume) to quantify methane evolved during the grafting. The resulting yellow powder was dried under vacuum (1.34 Pa) to yield 406 mg of **2**. Analysis by gas chromatography indicated the formation of 86 μ mol of methane during the grafting (1.0 nCH₄/nTa).

Reactivity of Propane on Solid 2. In a 352 mL volume reactor were added 67 mg of solid **2** (12.9 μ mol of Ta, 3.5%Ta) and propane

(40) Sanner, R. D.; Carter, S. T.; Bruton, W. J., Jr. *J. Organomet. Chem.* **1982**, *240*, 157–162.

(41) Oppolzer, W.; Mirza, S. *Helv. Chim. Acta* **1984**, *67*, 730–738.

(42) Hediger, S.; Meier, B. H.; Kurur, N. D.; Bodenhausen, G.; Ernst, R. R. *Chem. Phys. Lett.* **1994**, *223*, 283–288.

(43) Metz, G.; Wu, X.; Smith, S. O. *J. Magn. Reson., Ser. A* **1994**, *110*, 219–227.

(44) Bennett, A. E.; Rienstra, C. M.; Auger, M.; Lakshmi, K. V.; Griffin, R. G. *J. Chem. Phys.* **1995**, *103*, 6951–6958.

(45) Marion, D.; Wuethrich, K. *Biochem. Biophys. Res. Commun.* **1983**, *113*, 967–974.

(46) Bielecki, A.; Kolbert, A. C.; Levitt, M. H. *Chem. Phys. Lett.* **1989**, *155*, 341–346.

(47) Levitt, M. H.; Kolbert, A. C.; Bielecki, A.; Ruben, D. J. *Solid State Nucl. Magn. Reson.* **1993**, *2*, 151–163.

(48) Lesage, A.; Duma, L.; Sakellariou, D.; Emsley, L. *J. Am. Chem. Soc.* **2001**, *123*, 5747–5752.

(49) Michalowicz, A. *Logiciels pour la chimie*; Société Française de Chimie: Paris, 1991.

(50) Zabinsky, S. I.; Rehr, J. J.; Aukudinov, A.; Albers, R. C.; Eller, M. J. *Phys. Rev. B: Condens. Matter* **1995**, *52*, 2995–3009.

466 (495 Torr, 9.38 mmol). The reaction mixture was heated at 150 °C for
467 120 h, during which small aliquots were analyzed by GC and GC/MS.

468 **Reactivity of Propane on Solid 1.** In a 235 mL volume reactor
469 were added 60 mg of solid **1** (12.9 μ mol Ta, 3.9%_{Ta}) and propane (600
470 Torr, 7.59 mmol). The reaction mixture was heated at 150 °C for 120
471 h, during which small aliquots were analyzed by GC and GC/MS.

472 Conclusion

473 Generally, whether using [Ta(=CH*t*Bu)(CH₂*t*Bu)₃] or [Cp*Ta-
474 (CH₃)₄], the reaction with a silica partially dehydroxylated at
475 700 °C provides primarily the corresponding monosiloxy surface
476 complexes [(≡SiO)Ta(=CH*t*Bu)(CH₂*t*Bu)₂(≡SiOSi≡)] (**1a'**)
477 and [(≡SiO)Ta(CH₃)₃Cp*(≡SiOSi≡)] (**2a'**), by eliminating a
478 σ -bonded ligand as the corresponding alkane (H-CH₂*t*Bu or
479 H-CH₃). Moreover, when the metal is grafted, the coordination
480 number is increased by coordination of a pair of electrons from
481 the siloxane bridge, probably to stabilize the structure. In
482 particular, in the case of [Ta(=CH*t*Bu)(CH₂*t*Bu)₃], the surface
483 silanol [≡SiOH] reacts preferentially with the carbene, to yield
484 [(≡SiO)Ta(=CH*t*Bu)(CH₂*t*Bu)₂(≡SiOSi≡)], which is further
485 stabilized by an additional C-H agostic interaction. In the case
486 of [Cp*Ta(CH₃)₄], the size of the complex is such that after
487 grafting some surface silanols do not become accessible but
488 interact with adjacent Cp* ligands as evidenced by a strong
489 upfield shift of this signal.

490 In conclusion, the combined evidence presented here shows
491 the possibility for silica partially dehydroxylated at 700 °C to
492 act as a LX ligand in the Green formalism,^{3,51,52} rather than an
493 X ligand, as is the most commonly reported. Moreover, the
494 formation of well-defined species characterized at a molecular

495 level provides the possibility for one to probe mechanisms in
496 heterogeneous catalysis through structure-activity relationship.
497 In particular, in the case of alkane metathesis, the absence of
498 activity of [(≡SiO)Ta(CH₃)₃Cp*(≡SiOSi≡)] (**2a'**) and the
499 product selectivity when [(≡SiO)Ta(=CH*t*Bu)(CH₂*t*Bu)₂-
500 (≡SiOSi≡)] (**1a'**) was used as a catalyst precursor show that
501 the active site is required to be highly electrophilic, coordina-
502 tively unsaturated, and probably involves a metallacyclobutane
503 intermediate. We are currently trying to probe the other steps
504 of the mechanisms such as how the alkane is activated and how
505 the olefins are formed.

506 This insight was gained by the combined use of several
507 analytical techniques, with particular relevance given to the
508 necessity to complement more traditional spectroscopic data (IR,
509 one-dimensional solid-state NMR...) with data from techniques
510 such as EXAFS and multidimensional NMR spectroscopies.

511 **Acknowledgment.** M.C. and E.L.R. are grateful to the
512 ministry of education, research & technology, and BP Chemicals
513 for predoctoral fellowships, respectively. We thank M. El Eter
514 for providing helpful data on molecular tantalum complexes.
515 We thank B. M. Maunders for helpful discussions. We also wish
516 to thank Drs. V. Briois and S. Belin for their help in the
517 recording of the EXAFS data on XAS4/D44 at L.U.R.E., Orsay,
518 France (project n° CK 897-02). This work has also been
519 sponsored by BP Chemicals, the CNRS, ENS Lyon, and ESCPE
520 Lyon.

521 **Supporting Information Available:** NMR spectra. This
522 material is available free of charge via the Internet at
523 <http://pubs.acs.org>.

JA046486R

524

(51) Elschenbroich, C.; Salzer, A.; Eds. *Organometallics: A Concise Introduction*, Second, Revised Edition; VCH: New York, 1992.

(52) Green, M. L. H. *J. Organomet. Chem.* **1995**, *500*, 127-148.